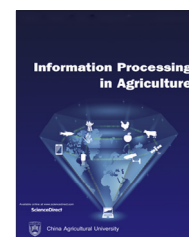


Available at www.sciencedirect.com

INFORMATION PROCESSING IN AGRICULTURE xxx (xxxx) xxx

journal homepage: www.elsevier.com/locate/inpa

Detection of leaf folder and yellow stemborer moths in the paddy field using deep neural network with search and rescue optimization

Chiranjeevi Muppala*, Velmathi Guruviah

SENSE Department, VIT University, Chennai, India

ARTICLE INFO

Article history:

Received 28 April 2020
Received in revised form
9 September 2020
Accepted 20 September 2020
Available online xxxx

Keywords:

Yellow stemborer
Leaf folder
Social ski-driver optimization
Search and rescue optimization
Deep neural network

ABSTRACT

In agriculture, insect pests must be identified at the initial stage of infestation to avoid their spread in the field. Leaf folders (*cnaphalocrocis medinalis*) and yellow stemborers (*scirpophaga incertulas*) are destructive pests of paddy crops, which are causing severe yield loss. Manual identification of insect pests in the crop is time-consuming, tedious, and ineffective. This paper focuses on a light trap based four-layer deep neural network with search and rescue optimization (DNN-SAR) method to identify leaf folders and yellow stemborers. Light traps are designed to lure the insects in the paddy field and the images of trapped insects are analyzed using the proposed detection method. In the DNN-SAR, images are contrast-enhanced using deer hunting algorithm, impulse noise is removed with fast average group filter, and segmented using social ski-driver optimization. The search and rescue optimization algorithm is used for the selection of optimal weights in the deep neural network, which has improved the convergence rate, lowered the complexity of learning, and improved the accuracy of detection. The proposed method outperformed the existing methods and achieved 98.29% pest detection accuracy.

© 2020 China Agricultural University. Production and hosting by Elsevier B.V. on behalf of KeAi. This is an open access article under the CC BY-NC-ND license (<http://creativecommons.org/licenses/by-nc-nd/4.0/>).

1. Introduction

Insect pests and diseases are some of the significant factors which are affecting crop yield in agriculture [1,2]. Pests are becoming immune to pesticides, making it difficult to contain them. As the pest population spreads in the field, controlling becomes very difficult, so early identification is critical. Rice (*Oryza sativa*) is the staple food for around half of the world's population and India is the second-largest producer of rice [3].

Rice crop was affected by hundreds of pests among them yellow stemborer (YSB) and leaf folder (LF) are major yield affecting insect pests [4,5] particularly in South Indian states. YSB larvae bore into the stems of the rice plant and destroy its panicles, resulting in loss of grains. LF larvae will reduce the photosynthesis process of the plants by eating the leaves. The traditional schemes of pest identification generally subject to visual identification by humans, which are error-prone and time-consuming. Machine vision methods can be used to automate the pest identification.

Various machine vision-based approaches have been proposed to identify different pests in the crops. Bernardes et al. [6] proposed an automatic classification of cotton diseases based on foliar symptoms from digital images. Wavelet

* Corresponding author.

E-mail addresses: muppala.chiranjeevi2016@vitstudent.ac.in (C. Muppala), velmathi.g@vit.ac.in (V. Guruviah).

Peer review under responsibility of China Agricultural University.
<https://doi.org/10.1016/j.inpa.2020.09.002>

2214-3173 © 2020 China Agricultural University. Production and hosting by Elsevier B.V. on behalf of KeAi.

This is an open access article under the CC BY-NC-ND license (<http://creativecommons.org/licenses/by-nc-nd/4.0/>).

transform was used for feature extraction and the SVM classifier was used for classifying different diseases. They achieved a classification accuracy of 71.4% for the ascochyta blight, 97.1% for the bacterial blight, and 80% for the ramularia disease. Turkoglu et al. [7] proposed a hybrid model based on the combination of the long short term memory(LSTM) network along with the pre-trained CNN models for the detection of apple pests and diseases. GoogleNet, DenseNet201, and AlexNet models were used for feature extraction whereas feature classification was done by SVM and LSTM classifiers. An accuracy of 99.2% was achieved with the LSTM classifier.

Qing et al. [8] proposed a method to identify white-backed planthoppers in paddy fields. The detection method used AdaBoost classifier, SVM classifier trained with Gabor and LBP features, and histogram of oriented gradients features for detecting the pests. They achieved 90.7% detection accuracy. Ding et al. [9] used pheromone pest traps to trap the codling moths (*Cydia pomonella*). The images captured from the trap were analyzed using CNN, to identify the moths and achieved an accuracy of 93.4%. Doitsidis et al. [10] developed an automated McPhail e-trap to detect and count olive fruit flies (*Bactrocera oleae*) in olive orchards. To attract the fruit flies, ammonium sulfate was filled in the trap. The trapped fruit flies images were then sent to a web-based system for analysis by the experts. Li et al. [11] proposed a crop pest recognition method to identify ten common species of crop pests using five deep convolutional neural networks (GoogLeNet, ResNet152, ResNet50, VGG-19, and VGG-16). GoogLeNet outperformed other models and achieved 96.67% identification accuracy. Hong et al. [12] proposed a method to detect *Spodoptera litura*, *Spodoptera exigua*, and *Helicoverpa assulta* moths in pheromone trap images using seven deep learning object detection methods (Faster R-CNN ResNet50, Faster R-CNN ResNet101, Faster R-CNN Inception v2, R-FCN ResNet101, Retinanet ResNet50, SSD Inception v2, and, Retinanet Mobile v2). Faster R-CNN ResNet101 performed better with an accuracy of 90.25%. Alves et al. [13] proposed a deep residual network ResNet34* to classify major cotton pests and compared the performance with Linear binary features (LBP)- SVM, AlexNet, ResNet34, and ResNet50. Proposed ResNet34* classified the cotton pests better and achieved an overall accuracy of 98.1%.

Most of the existing methods use machine vision for the identification of pests by analyzing the images of plant leaves. Because of the complex background of the leaves detection accuracy was poor. Furthermore, the automation of the whole process is inadequate. By deploying light traps in the field and identifying images of pests captured from the light trap will improve the pest detection efficiency so that pest control strategies can be implemented quickly. As the dimensions of YSB and LF moths are ranging from 15 to 20 mm, efficient optimization algorithms must be chosen to achieve better detection accuracy.

The present work focuses on a four-layer deep neural network (DNN) which has contrast enhancement, impulse noise removal, segmentation, and DNN with search and rescue optimization algorithm (SAR) in the pest detection module. Deer hunting optimization (DHO) for contrast enhancement and social ski-driver (SSD) algorithm for segmentation was

chosen after evaluating various popular algorithms. Fast averaging peer-group filter (FAPGF) was used for removing the impulse noise from the test image. In the last layer, a new hybrid object detection algorithm namely deep neural network with search and rescue optimization was used for detecting LF and YSB from the test image. Finally, the pest detection accuracy of the proposed method was compared with the existing detection methods. The basic block diagram of the proposed DNN-SAR pest detection method was shown in Fig. 1.

2. Materials and methods

2.1. Image acquisition

Pest samples were collected from the paddy field using proposed insect light traps as shown in Fig. 2a. Four different light sources [14] with wavelengths of 365 ± 5 nm (ultraviolet), 405 ± 5 nm (violet), 465 ± 5 nm (blue), and 525 ± 5 nm (green) were used in the traps. The light sources are made of SMD-LED tapes rolled around 1-foot long, 1-inch diameter tubes as shown in Fig. 2b and they are powered by a 12AH 12 V DC battery. Beneath the light source, a funnel was attached to a plastic container that has a black-coated plate beneath it to collect the pests fallen inside it. The trapped pests in the container are shown in Fig. 2c. The trapped pest images are captured with a 20MP Canon IXUS 285 HS digital camera with a 12x optical zoom. All the images were formatted to .jpeg with 256 X 256-pixel resolution for consistency in the dataset.

2.2. Contrast enhancement

In image processing, contrast enhancement is performed to improve the quality of an image. Global contrast enhancement techniques like histogram equalization and global stretching are widely used for contrast enhancement, but when the image has large spatial variation in contrast, optimal results can't be obtained. To overcome this, local contrast enhancement methods like the DHO algorithm [15], whale optimization algorithm (WOA) [16], particle swarm optimization (PSO) [17], grey wolf optimizer (GWO) [18], group search optimizer (GSO) [19], artificial bee colony optimization (ABC) [20], etc., can be used. DHO algorithm was chosen for contrast enhancement of the test image, which was motivated by the hunting behavior of the human towards the deer. The hunting of deer depends on the movement of the leader and the successor. In the initial stage of DHO, the population and the parameters like wind angle(θ) and position angle(φ_j) are initialized, where the wind and position angle are determined by

$$\theta_j = 2 * \pi * r \quad \text{and} \quad \varphi_j = \pi + \theta_j \quad (1)$$

(a) Position for the leader

After defining the best positions, the encircling behavior is given by

$$Z_{i+1} = Z^l - Y * q * |P * Z^l - Z_i| \quad (2)$$

Where Z_i & Z_{i+1} are the present and next positions, Y and P are the coefficient vectors, q is a random number ranges from 0 to

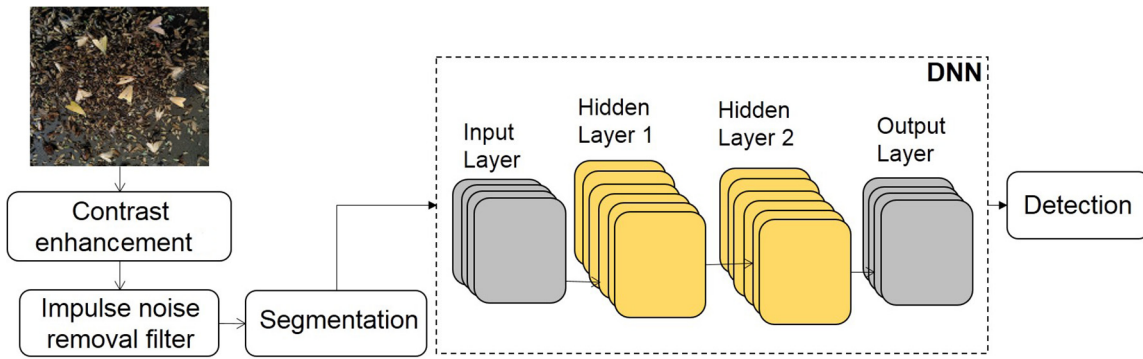


Fig. 1 – Basic block diagram of the proposed DNN-SAR pest detection method.



(a)



(b)



(c)

Fig. 2 – a) Light traps deployed in the paddy field b) Four light sources used in the traps c) Trapped pests in the collector plate.

2 and Z^L is the leader position which is the first best position of the hunter.

$$Y = \frac{1}{4} \log \left[t + \frac{1}{t_{\max}} \right] b \quad \text{and} \quad P = 2 * c \quad (3)$$

Here t_{\max} represents the maximum value of iteration, b and c are arbitrary numbers ranges in the interval $[-1, 1]$ and $[0, 1]$.

(b) Propagation through position angle (PA)

By considering the PA the resultant space is modified. The visualization angle for deer is determined by,

$$w_i = \frac{\pi}{8} * r \quad (4)$$

The position angle is updated using

$$\varphi_{i+1} = \varphi_i + d_i \quad \text{where} \quad d_i = \theta_i - w_i \quad (5)$$

The position update equation is

$$Z_{i+1} = Z^L - q * |\text{Cos}(\varphi_{i+1}) * Z^L - Z_i| \quad (6)$$

(c) Position of the successor: For making a global search

for the position updation, the successor position is taken.

$$Z_{i+1} = Z^S - Y * q * |P * Z^S - Z_i| \quad (7)$$

Where Z^S is the successor position i.e succeeding hunter position.

2.3. Impulsive noise removal using FAPG filter

FAPG filter aims to eliminate the unwanted impulsive noises of the contrast-enhanced image. In FAPGF [21], the center pixel's grade of membership is expressed in terms of peer group size. FAPGF consists of two steps, pixel inspection, and replacement. Pixel inspection estimates the grade of membership of the center pixel of the local window to its neighborhood. Peer group size represents the total close neighbors of the center pixel. The total pixels n_k from W enclosed in a sphere of radius r centered at pixels $_k$ is represented as the peer group size.

$$n_k = \# \{y_j \in W : \|y_k - y_j\| < r\} \quad (8)$$

Here # represents the cardinality and $\|\cdot\|$ is the Euclidean norm.

If the size of the peer group of the center pixel is less than 1 then it is treated as outliers and if the size is greater than 1 then it is preserved. All the outliers are replaced by the weighted average filter (WAF) in the pixel replacement step. WAF is checked by analyzing the dimension of the peer groups of the testers which are in neighborhood relation with the proposed pixel. The output Z_1 of WAF is

$$z_1 = \frac{1}{\sum_{i=2}^n w_i} \sum_{i=2}^n w_i * x_i \quad (9)$$

where

$$w_i = \frac{\eta_i}{\sum_{i=2}^n \eta_i}; \eta_i = n_i^\gamma \text{ and } \gamma > 0 \quad (10)$$

x_i is the i_{th} pixel, $\gamma > 0$ is the secondary parameter influencing the quality of results.

After contrast enhancement and impulse noise reduction, the image was segmented using social ski-driver optimization.

2.4. Segmentation

For insect identification and detection, the segmentation of individual insects from the background is necessary. To detect the object of interest that is YSB and LF from the image, the thresholding technique was used. For separating multiple objects from the background, multilevel Otsu thresholding was selected. The optimal value of the threshold was selected using the SSD algorithm. Consider a gray level image I to be segmented consisting of $K + 1$ classes. To partition the image into sub-regions, k threshold values (h_1, h_2, \dots, h_k) are required. The class of image is represented as

$$\begin{aligned} I_0 &= \{f(i, j) \in I | 0 \leq f(i, j) \leq h_1 - 1\} \\ I_1 &= \{f(i, j) \in I | h_1 \leq f(i, j) \leq h_2 - 1\} \\ &\dots \\ I_k &= \{f(i, j) \in I | h_k \leq f(i, j) \leq N - 1\} \end{aligned} \quad (11)$$

Where $f(i, j)$ is the gray level of the pixel (i, j) . The threshold value is identified by maximizing the variance.

$$h_1^*, h_2^*, \dots, h_k^* = \max_{t_1, \dots, t_k} F(h_1, t_1, \dots, h_k) \quad (12)$$

Where

$$F = \sum_{i=0}^k A_i (\eta_i - \eta_1)^2; A_i = \sum_{j=t_i}^{t_{i+1}-1} P_j \quad (13)$$

$$\eta_i = \sum_{j=t_i}^{t_{i+1}-1} i \frac{P_j}{A_j} \quad \text{where } P_i = h(i)N_p \quad (14)$$

Here P_i is the probability and $h(i)$ is the frequency of the i^{th} gray level, N_p is the total number of pixels and η is the mean intensity.

SSD was proposed by Tharwat et al. [22] which imitates the paths that ski-drivers take down the hill. The SSD optimization is applied in segmentation for the optimal selection of the threshold value. In SSD randomly initialize the position (Y_i) and the user selects the number of agents. By adding a velocity constraint to their old positions, all agents update their position, and it is given as

$$Y_i^{t+1} = Y_i^t + U_i^t \quad (15)$$

The velocities of the agents are modified using

$$U_i^{t+1} = \begin{cases} d * \text{Sin}(s_1)(P_i^t - Y_i^t) + \text{Sin}(s_1)(M_i^t - Y_i^t) & \text{if } s_2 \leq 0.5 \\ d * \text{Cos}(s_1)(P_i^t - Y_i^t) + \text{Cos}(s_1)(M_i^t - Y_i^t) & \text{if } s_2 > 0.5 \end{cases} \quad (16)$$

The d is a parameter which is used to make a balance between exploration and exploitation and d is given by

$$d^{t+1} = \mu * d^t \quad (17)$$

here t is the iteration and $0 < \mu < 1$, s_1 and s_2 are in the range 0 to 1. The best solution of the i^{th} agent is represented as P_i and M_i is the mean global solution of the entire population, and it is found using as in the Grey wolf optimizer.

The mathematical representation is given as,

$$M_i^t = \frac{Y_x + Y_\beta + Y_\gamma}{3} \quad (18)$$

here $Y_x, Y_\beta \& Y_\gamma$ are the best three solutions.

2.5. Detection

For detecting the YSB and LF, an optimized DNN using the SAR algorithm was proposed. A DNN is an artificial neural network that has input, hidden, and output layers. The hidden layer performs a set of non-linear functions and it is represented as

$$Z = \text{sig}(W * x + \text{bias}) \quad (19)$$

Where x is the input of each node, W and bias are the weight and bias vector respectively and sig represents the sigmoid activation function, i.e. $\frac{1}{1+e^{-x}}$.

In our proposed optimized DNN, two hidden layers are considered and to minimize the mean absolute error (MAE) of the DNN, optimal selection of the weight matrices was necessary so, here SAR was utilized. The structure of DNN was shown in Fig. 3. Shabani et al. [23] proposed SAR, which is motivated by the investigations carried out by humans during search and rescue operations. The search and rescue operation has mainly two phases, i.e. social phase and individual phase. During the search process, group members gather the clues.

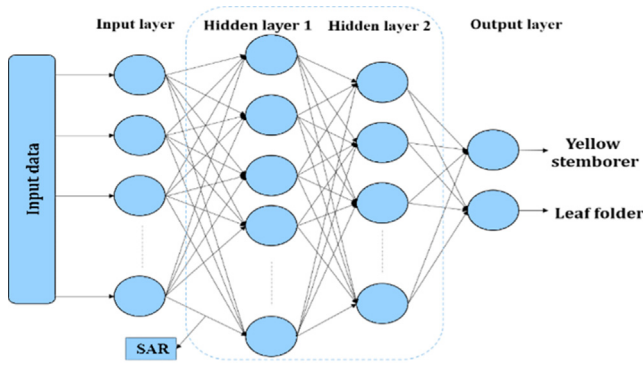


Fig. 3 – Proposed DNN structure.

The clues left during the search by the group members are stored in the memory matrix (O) whereas the human's positions are stored in the position matrix (W). The clue matrix B with size $N \times D$, which contains the left clues and the human's positions are represented as

$$B = \begin{bmatrix} W \\ O \end{bmatrix} = \begin{bmatrix} W_{11} & \cdots & W_{1D} \\ \vdots & \ddots & \vdots \\ W_{N1} & \cdots & W_{ND} \\ O_{11} & \cdots & O_{1D} \\ \vdots & \ddots & \vdots \\ O_{N1} & \cdots & O_{ND} \end{bmatrix} \quad (20)$$

The two phases of human search are modeled as follows.

i) *Social phase*:- The search direction is given by $SD_i = (W_i - B_k)$ where $k \neq i$. The new solution is generated using the equation

$$W'_{ij} = \begin{cases} \begin{cases} B_{ij} + r_1(W_{ij} - B_{ij}), & \text{if } f(B_i) > f(W_i) \\ W_{ij} + r_1(W_{ij} - B_{ij}), & \text{otherwise} \end{cases} & \text{if } r_2 > SE \\ W_{ij} & \text{otherwise} \end{cases} \quad (21)$$

Here $f(B_i)$ & $f(W_i)$ are the fitness function values for B_i & W_i , r_1 and r_2 are random numbers in the range $[-1, 1]$ and $[0, 1]$, SE is algorithm parameter ranging between 0 and 1.

ii) *Individual Phase*:- Based on the current position humans identify their new position and the new position of the i^{th} human is given by,

$$W'_i = W_i + r_3(B_k - B_m), \quad i \neq k \neq m \quad (22)$$

All the solutions should locate in the solution space, if the new position is outer the solution space then it is improved using the equation

$$W^{\wedge}_{ij} = \begin{cases} \frac{W_{ij} + W_j^{\max}}{2} & \text{if } W^{\wedge}_{ij} > W_j^{\max} \\ \frac{W_{ij} + W_j^{\min}}{2} & \text{if } W^{\wedge}_{ij} < W_j^{\min} \end{cases} \quad (23)$$

Where W_j^{\max} and W_j^{\min} are the maximum and minimum of the threshold. The efficiency of finding the global optimal solution is increased by the given memory updating equations

$$ME_n = \begin{cases} W_i & \text{if } f(W'_i) > f(W_i) \\ ME_n & \text{otherwise} \end{cases} \quad (24)$$

$$W_i = \begin{cases} W'_i & \text{if } f(W'_i) > f(W_i) \\ W_i & \text{otherwise} \end{cases} \quad (25)$$

Where ME_n is the n^{th} stored clue position in the memory matrix and n is a random integer number ranging between 1 and N .

In the clue search process, if better clues are not found around the current position after a certain number of searches, human goes to a new position. To model this, at first, an unsuccessful search number (USN) is set to 0 for each human.

$$USN_i = \begin{cases} USN_i + 1 & \text{if } f(W'_i) > f(W_i) \\ 0 & \text{otherwise} \end{cases} \quad (26)$$

When the USN value is higher than the maximum unsuccessful search number, the human got a random position in the search space using Eq. (27), and the value of USN_i is set to 0 for that human.

$$w_{ij} = w_j^{\min} + r_4(w_j^{\max} - w_j^{\min}); j = 1, \dots, D \quad (27)$$

Where r_4 ranges in the interval 0 and 1.

3. Results

The trapped YSB and LF moths separated from the light trap and placed in various backgrounds to capture the images. 300-YSB and 269-LF images were collected from the trap which were then divided into two sets, one for training and another for validation. The training dataset was prepared with 80% of collected images and the remaining 20% used for validation. Augmentation was applied over the images to increase the size of the dataset. There are various image augmentation approaches such as affinity transformation, perspective transformation, flipping, scaling, translation, and simple rotation out of which simple rotation (pest images were rotated by 90° , 180° , and 270°) was chosen, thus the total images in the dataset increased from 569 to 2326 as shown in Table 1.

The sample dataset images of LF and YSB are shown in Fig. 4a & b. The test image captured from the light trap's collector plate as shown in Fig. 5a was sent through the proposed 4-layer detection process. In the first layer, the contrast of the input test image was enhanced using DHO and the corresponding contrast-enhanced image was shown in Fig. 5b. The performance of the DHO contrast enhancement was evaluated with parameters like peak signal to noise ratio (PSNR), absolute mean brightness error (AMBE) [24], and contrast improvement index (CII) [25,26]. The higher value of PSNR indicates better image quality, lower value of AMBE indicates better preserving the original brightness of the image, and higher CII indicates an increase in the contrast generated by the methods. DHO enhanced the test image contrast with high PSNR, low AMBE, and high CII values when compared with PSO, GWO, and WOA methods as shown in Table 2. The contrast-enhanced image sent through the FAPG filter to reduce impulse noise and the corresponding noise removed image was shown in Fig. 5c.

In the third layer, image segmentation was performed on the FAPGF output image using the SSD algorithm. The segmented output image was shown in Fig. 5d. The segmentation performance of the SSD, PSO, and GWO were compared with respect to the probabilistic rand index (PRI) [27,28], global

Table 1 – No. of YSB and LF images in the dataset.

Dataset	LF	YSB	Total
<i>Before augmentation</i>			
Training	250	224	474
Validation	50	45	95
Total	300	269	569
<i>After augmentation</i>			
Training	1000	896	1896
Validation	250	180	430
Total	1250	1076	2326



(a) Leaf folders



(b) Yellow stemborers

Fig. 4 – Sample images from the dataset.

consistency error (GCE) [29], boundary displacement error (BDE) and variations of information (VI) [30,31]. PRI counts the correctness in segmentation and its value is between 0 and 1, where value nearer to 1 indicates better similarity between two segments. GCE measures the relative consistency between two alternative segmentation solutions. BDE measures the average displacement error of boundary pixels of two segments. VI measures the amount of randomness in one segmentation, which cannot be explained by the other.

SSD based segmentation was better than other segmentation methods, with higher PRI and lower GCE, BDE, and VI as shown in Table 3. The segmented image as shown in Fig. 5d was sent to the DNN-SAR algorithm to locate and identify

YSB and LF moths in the test image. The final output image has bounding boxes over the moths as shown in Fig. 5e, where yellow bounding box represents YSB and the red bounding box represents LF. The performance of DNN-SAR was compared with AlexNet, GoogleNet, and ResNet50 with the same inputs. The performance comparison of DNN-SAR and the existing methods was shown in Table 4 and the comparison plots were shown in Fig. 6.

The proposed system achieved 98.29% accuracy, with 97.85% precision. The DNN-SAR attained 98.3% F1 score, 98.75% Recall, and 0.0125 false-negative rate (FNR). DNN-SAR got better accuracy than other models, whereas ResNet50 was second best with the accuracy of 95.47%. In the detection of YSB and LF moths from the light trap images, our proposed DNN-SAR performed better in terms of all performance parameters when compared with existing methods.

4. Conclusion

In this paper, a four-layer DNN-SAR pest detection method was proposed to identify yellow stemborer, and leaf folder moths in the paddy field. Four light traps with different wavelength light sources were designed in the paddy field for collecting YSB and LF images. In the first layer of the proposed method, DHO algorithm was chosen for image contrast enhancement after comparing the performance parameters like PSNR, AMBE, and CII of DHO, PSO, GWO, and WOA algorithms. In the second layer, FAPG filter was used to remove impulse noise in the image. In the third layer, the image was segmented by selecting the optimal threshold values with SSD algorithm. The SSD algorithm was chosen after comparing PRI, GCE, BDE, and VI parameters of PSO, GWO, and SSD optimization algorithms. In the final layer, optimal weights in the neural network were chosen with SAR optimization, which has improved the convergence rate and reduced the complexity of learning. With the proper selection of optimization algorithms in the pest detection process, the proposed method has achieved 98.29% accuracy with 97.85% precision and attained recall, F1 score, and FNR of 98.75%, 98.30%, and 0.0125 respectively. The DNN-SAR pest detection method can be further extended to other paddy pests so that all the major paddy pests can be identified. Besides, the light trap based pest trapping and automation of the entire detection process in real-time can help farmers to take swift action against the crop-damaging pests.

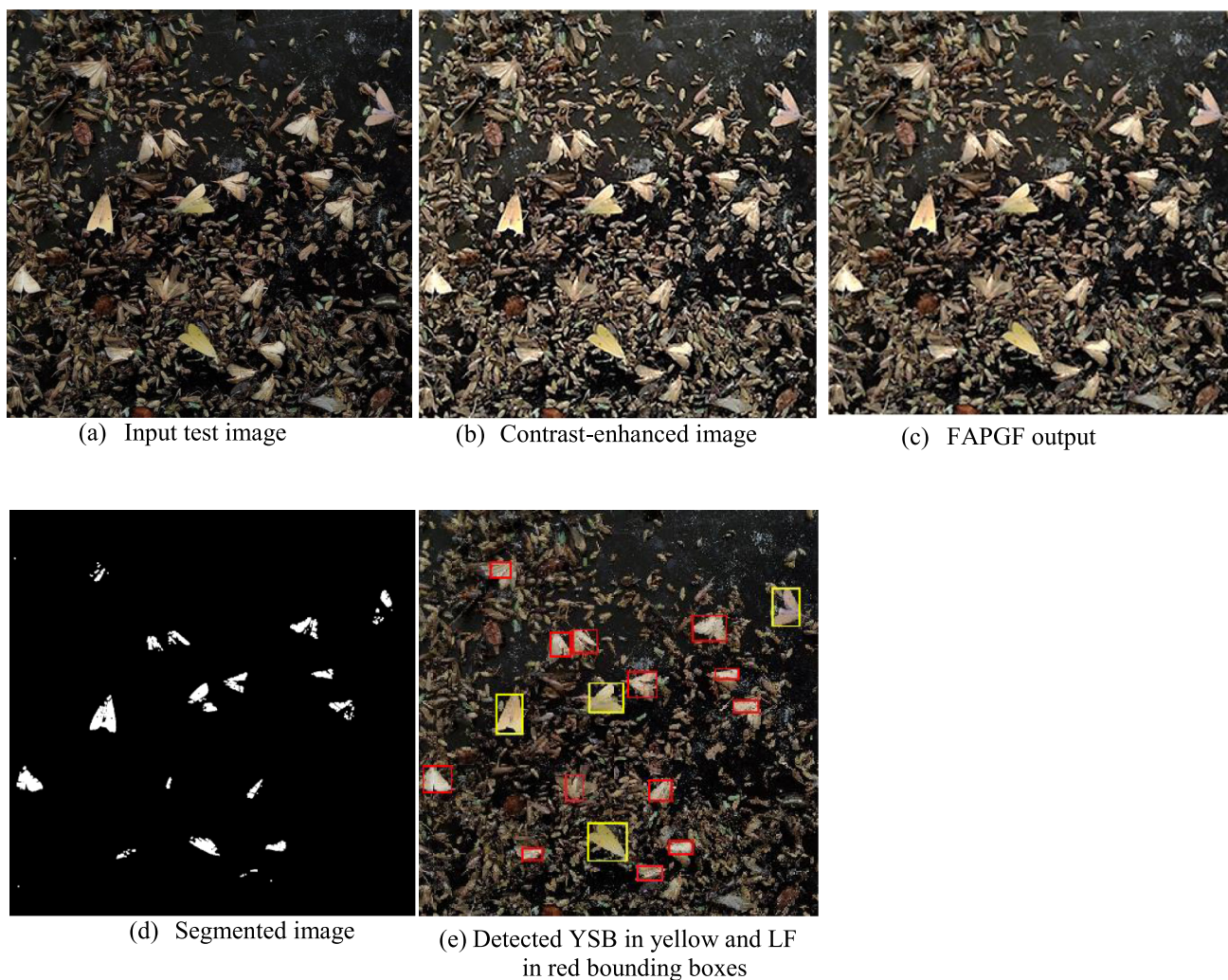


Fig. 5 – Step by step results of the proposed method.

Table 2 – Performance of different contrast enhancement techniques.

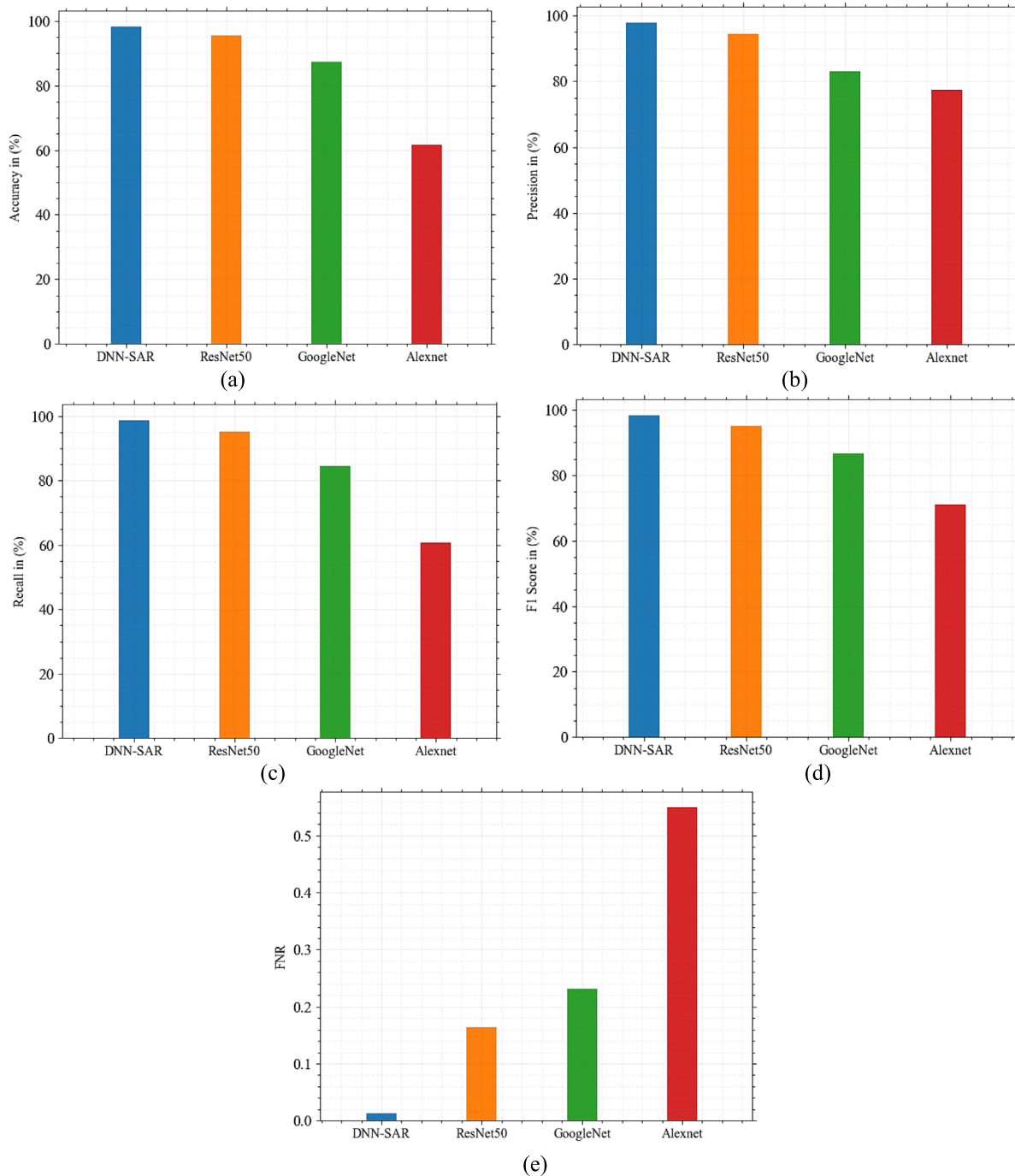
Parameters	PSO	GWO	WOA	DHO
PSNR	15.28	16.02	19.1	25.46
AMBE	3.09	7.06	5.21	2.40
CII	1.3022	0.8898	2.3457	4.6595

Table 3 – Performance of different segmentation techniques.

Parameters	PSO	GWO	SSD
PRI	0.7673	0.6349	0.9231
GCE	0.3514	0.3288	0.2562
BDE	0.4703	0.5178	0.1986
VI	3.5013	2.8223	2.3930

Table 4 – Performance comparison of DNN-SAR and existing methods.

Method	Accuracy	Precision	Recall	F ₁ Score	FNR
DNN-SAR	98.29	97.85	98.75	98.30	0.0125
ResNet50	95.47	94.32	95.26	94.95	0.1641
GoogleNet	87.32	82.14	84.60	86.51	0.2312
Alexnet	61.7	77.47	60.79	70.94	0.55

**Fig. 6 – Performance comparison graphs of proposed and existing methods (a) Accuracy (b) Precision (c) Recall (d) F1 score (e) FNR.**

Declaration of Competing Interest

The authors declare that they have no known competing financial interests or personal relationships that could have appeared to influence the work reported in this paper.

Acknowledgments

We express our sincere thanks to Dr. R.P. Soundararajan (Tamilnadu agricultural university, Trichy) for his valuable suggestions in identifying paddy pests and his valuable guidance for maintaining sufficient leaf folder and yellow stem-borer moths in the test fields.

REFERENCES

- [1] Oerke EC. Crop losses to pests. *J Agric Sci* 2006;144(1):31–43.
- [2] Zimmermann H.G., Granata G. Insect pests and diseases. In: Nobel P. *Cacti: biology and uses*. USA: California Scholarship Online; 2002. p. 235–254.
- [3] Hegde S, Hegde V. Assessment of Global Rice Production and Export Opportunity for Economic Development in Ethiopia. *Int J Sci Res* 2013;2(6):2319–7064.
- [4] Maqbool SB, Husnain T, Riazuddin S, Masson L, Christou P. Effective control of yellow stem borer and rice leaf folder in transgenic rice indica varieties Basmati 370 and M 7 using the novel δ -endotoxin cry2A *Bacillus thuringiensis* gene. *Mol Breed* 1998;4(6):501–7.
- [5] Muralidharan K, Pasalu IC. Assessments of crop losses in rice ecosystems due to stem borer damage (Lepidoptera: Pyralidae). *Crop Prot* 2006;25(5):409–17.
- [6] Bernardes AA, Rogeri JG, Oliveira RB, Marranghello N, Pereira AS, Araujo AF, et al. Identification of foliar diseases in cotton crop. In: *Topics in Medical Image Processing and Computational Vision*. p. 67–85.
- [7] Turkoglu M, Hanbay D, Sengur A. Multi-model LSTM-based convolutional neural networks for detection of apple diseases and pests. *J Ambient Intell Humaniz Comput* 2019:1–11.
- [8] Qing YA, Chen GT, Zheng WA, Zhan C, Yang BJ, Jian TA. Automated detection and identification of white-backed planthoppers in paddy fields using image processing. *J Integr Agric* 2017;16(7):1547–57.
- [9] Ding W, Taylor G. Automatic moth detection from trap images for pest management. *Comput Electron Agric* 2016;123:17–28.
- [10] Doitsidis L, Fouskitakis GN, Varikou KN, Rigakis II, Chatzichristofis SA, Papafilippaki AK, et al. Remote monitoring of the *Bactrocera oleae* (Gmelin) (Diptera: Tephritidae) population using an automated McPhail trap. *Comput Electron Agric* 2017;137:69–78.
- [11] Li Y, Wang H, Dang LM, Sadeghi-Niaraki A, Moon H. Crop pest recognition in natural scenes using convolutional neural networks. *Comput Electron Agric* 2020;169 105174.
- [12] Hong SJ, Kim SY, Kim E, Lee CH, Lee JS, Lee DS, et al. Moth Detection from Pheromone Trap Images Using Deep Learning Object Detectors. *Agriculture* 2020;10(5):170.
- [13] Alves AN, Souza WS, Borges DL. Cotton pests classification in field-based images using deep residual networks. *Comput Electron Agric* 2020;174 105488.
- [14] Shimoda M, Honda K ichiro. Insect reactions to light and its applications to pest management. *Appl Entomol Zool* 2013; 48:413–21.
- [15] Brammya G, Praveena S, Ninu Preetha NS, Ramya R, Rajakumar BR, Binu D. Deer Hunting Optimization Algorithm: A New Nature-Inspired Meta-heuristic Paradigm. *Comput J* 2019.
- [16] Mirjalili S, Lewis A. The whale optimization algorithm. *Adv Eng Softw* 2016;95:51–67.
- [17] Tian DP, Li NQ. Fuzzy particle swarm optimization algorithm. In: 2009 International Joint Conference on Artificial Intelligence. IEEE; 2009. p. 263–7.
- [18] Mirjalili S, Mirjalili SM, Lewis A. Grey wolf optimizer. *Adv Eng Softw* 2014;69:46–61.
- [19] He S, Wu QH, Saunders JR. Group search optimizer: an optimization algorithm inspired by animal searching behavior. *IEEE Trans Evol Comput* 2009;13(5):973–90.
- [20] Karaboga D, Basturk B. Artificial bee colony (ABC) optimization algorithm for solving constrained optimization problems. In: *International fuzzy systems association world congress*. Springer; 2007. p. 789–98.
- [21] Malinski L, Smolka B. Fast averaging peer group filter for the impulsive noise removal in color images. *J Real-Time Image Process* 2016;11(3):427–44.
- [22] Tharwat A, Gabel T. Parameters optimization of support vector machines for imbalanced data using social ski driver algorithm. *Neural Comput Appl* 2019:1–4.
- [23] Shabani A, Asgarian B, Gharebaghi SA, Salido MA, Giret A. A New Optimization Algorithm Based on Search and Rescue Operations. *Math Probl Eng* 2019.
- [24] Patel O, Maravi YP, Sharma S. A comparative study of histogram equalization based image enhancement techniques for brightness preservation and contrast enhancement. *arXiv preprint arXiv:1311.4033*, 2013.
- [25] Puniani S, Arora S. Performance evaluation of image enhancement techniques. *Int J Signal Process, Image Process Pattern Recogn* 2015;8(8):251–62.
- [26] Wang Z, Wang K, Yang F, Pan S, Han Y, Zhao X. Image enhancement for crop trait information acquisition system. *Inform Process Agric* 2018;5(4):433–42.
- [27] Unnikrishnan R, Pantofaru C, Hebert M. Toward objective evaluation of image segmentation algorithms. *IEEE Trans Pattern Anal Mach Intell* 2007;29(6):929–44.
- [28] Peng B, Zhang L, Zhang D. A survey of graph theoretical approaches to image segmentation. *Pattern Recogn* 2013;46(3):1020–38.
- [29] Martin D, Fowlkes C, Tal D, Malik J. A database of human segmented natural images and its application to evaluating segmentation algorithms and measuring ecological statistics. In: *Proceedings Eighth IEEE International Conference on Computer Vision*. p. 416–23.
- [30] Sathya B, Manavalan R. Image segmentation by clustering methods: performance analysis. *Int J Comput Appl* 2011;29(11):27–32.
- [31] Manavalan R, Thangavel K. TRUS image segmentation using morphological operators and DBSCAN clustering. In: *World Congress on Information and Communication Technologies*. IEEE; 2011. p. 898–903.